

α Annealing of Ant Colony Optimization in the infinite-range
Ising model

Shintaro Mori* and Taiyo Shimizu†

*Graduate school of Science and Technology, Hirosaki University,
Bunkyo-cho 3, Hirosaki, Aomori 036-8561, Japan*

Masato Hisakado‡

*Nomura Holdings Inc.,
Otemachi 2-2-2, Chiyoda-ku,
Tokyo 100-8130, Japan*

Kazuaki Nakayama§

*Department of Mathematical Sciences,
Faculty of Science, Shinshu University,
Asahi 3-1-1, Matsumoto, Nagano 390-8621, Japan*

(Dated: July 30, 2024)

Abstract

Ant colony optimization (ACO) leverages the parameter α to modulate the decision function's sensitivity to pheromone levels, balancing the exploration of diverse solutions with the exploitation of promising areas. Identifying the optimal value for α and establishing an effective annealing schedule remain significant challenges, particularly in complex optimization scenarios. This study investigates the α -annealing process of the linear Ant System within the infinite-range Ising model to address these challenges. Here, "linear" refers to the decision function employed by the ants. By systematically increasing α , we explore its impact on enhancing the search for the ground state. We derive the Fokker-Planck equation for the pheromone ratios and obtain the joint probability density function (PDF) in stationary states. As α increases, the joint PDF transitions from a mono-modal to a multi-modal state. In the homogeneous fully connected Ising model, α -annealing facilitates the transition from a trivial solution at $\alpha = 0$ to the ground state. The parameter α in the annealing process plays a role analogous to the transverse field in quantum annealing. Our findings demonstrate the potential of α -annealing in navigating complex optimization problems, suggesting its broader application beyond the infinite-range Ising model.

I. INTRODUCTION

Ant colony optimization (ACO) is a popular meta-heuristic of swarm intelligence for approximating solutions to combinatorial optimization problems [1, 2]. Inspired by the foraging behavior of ant colonies [3–8], ACO employs simple agents, known as 'ants,' that search for the optimal solution through a combination of random search and indirect communication. This stigmergic communication involves ants depositing 'pheromone' following the construction and evaluation of a candidate solution, with the pheromone quantity reflecting the solution's quality, thereby guiding solution construction. ACO's effectiveness has been demonstrated across numerous *NP-hard* combinatorial optimization problems, with its success largely attributable to the cooperative interactions among ants via pheromones [9–12].

* shintaro.mori@hirosaki-u.ac.jp

† h24ms110@hirosaki-u.ac.jp

‡ hisakadom@yahoo.co.jp

§ nakayama@math.shinshu-u.ac.jp

Following ACO's practical successes, several studies have elucidated its underlying mechanisms. Meuleau and Dorigo illustrated the strong relationship between ACO algorithms and stochastic gradient descent, demonstrating that specific ACO forms probabilistically converge to a local optimum [13]. Here, 'convergence' implies ants consistently constructing the same solution in ACO. Stützle and Dorigo provided proof of convergence for a class of ACO systems to the globally optimal solution [14], a finding further substantiated by Gutjahr's proof, which drew parallels with the convergence of simulated annealing [15, 16].

For ACO algorithm performance enhancement, controlling the diversity of candidate solutions is paramount [17–19]. Achieving an optimal balance between exploration (solution diversity) and exploitation (effective use of available solutions) requires meticulously designed convergence dynamics. Premature convergence can restrict exploration to a narrow search space segment, while excessively slow convergence may render the search process inefficient.

Meyer has emphasized the critical role of the algorithmic parameter α in controlling diversity [19–21]. α determines how the choice function depends on the pheromone amount x , represented as x^α . A low α value encourages ants to explore broadly, while a high α focuses the search more narrowly, similar to the role of temperature in simulated annealing. Adjusting α allows for a desirable balance between exploration and exploitation. The significance of noise in ACO has also been emphasized using stochastic differential equations in both static and dynamic environments [19, 21–23]. Ants respond to a two-choice question, and the noisy communication among ants prevents them from selecting suboptimal choices.

This paper explores the α -annealing process of ACO within the infinite-range Ising model. Here, α -annealing refers to a systematic method of gradually increasing α to balance the trade-off between exploration and exploitation. We adopt a linear decision function and explore the system through stochastic differential equations (SDEs). We derive the stationary solution of the Fokker-Planck equation for the pheromone ratios. Our analysis predicts a transition from a mono-modal joint probability density function (PDF) to a multi-modal one upon α surpassing a critical threshold (α_c). The trajectory of the stationary states induced by changes in α bridges the trivial solution and the global minimum of the homogeneous fully connected Ising model. The parameter α in the annealing process plays a role analogous to the transverse field in quantum annealing [24].

The organization of the paper is as follows: Section II introduces our ACO model that

searches for the ground state of the infinite-range Ising model. We adopt an Ant System (AS) with a linear decision function, which is the simplest formulation of the Ant Colony Optimization system. In Section III, we derive the SDEs for the pheromone ratios and obtain the stationary state of the joint PDF. Section IV studies the transition of the PDF for the homogeneous fully connected Ising model. The results are supported by numerical simulation in Section V. The probability of finding the ground state is maximized in the α -annealing process. Finally, Section VI summarizes our findings.

II. LINEAR ANT SYSTEM AND GROUND STATE SEARCH OF ISING MODEL

We address the problem of identifying the ground state of the Ising model, characterized by N binary variables $\{X(i) \in \{0, 1\}, i = 1, \dots, N\}$ [25]. The system's energy is defined as

$$E[\{X(i)\}] = - \sum_i h(i)(2X(i) - 1) - \frac{1}{N-1} \sum_{i,j,i \neq j} J(i,j)(2X(i) - 1)(2X(j) - 1). \quad (1)$$

In this model, $J(i, j) \in \mathbb{R}$ signifies the exchange interaction strength, and $h(i) \in \mathbb{R}$ represents the external field. Without loss of generality, we can assume $J(i, j) = J(j, i)$ and $h(i) \geq 0$. The Ising-lattice gas transformation $\sigma(i) = 2X(i) - 1$ maps the binary variables $\{X(i) \in \{0, 1\}, i = 1, \dots, N\}$ to Ising spin variables $\{\sigma(i) \in \{\pm 1\}, i = 1, \dots, N\}$. At thermal equilibrium, the joint probability distribution of $\{X(i)\}$ aligns with the Boltzmann weight, scaled as $\propto e^{-\beta E[\{X(i)\}]}$, where β is the inverse temperature. A positive external field ($h(i) > 0$) biases towards $X(i) = 1$, and a positive exchange interaction ($J(i, j) > 0$) encourages alignment, i.e., $X(i) = X(j)$.

Considering the homogeneous scenario where $J(i, j) = J$ and $h(i) = h$, the model is a homogeneous fully connected Ising model, where all variables interact equally. The ground state for $h > 0$ is uniformly $X(i) = 1$, with the energy being $-N(J + h)$. At $h = 0$, two ground states exist with the ground state energy $-NJ$: $X(i) = 1$ for all i and $X(i) = 0$ for all i . The external field breaks the degeneracy and the energy difference between these states for $h \neq 0$ is $2Nh$. The energy, given the magnetization $m = \sum_i (2X(i) - 1)/N$, is $-N(hm + Jm^2)$. The energy barrier from $m = -1$ to $m = 1$ is $N(J - h)$ and makes the ground state discovery ($m = 1$) challenging if $m = -1$ is initially found, especially when $J \gg h$ and $h > 0$.

In the Ant System (AS) described in this paper, ants sequentially search for the ground

state of the Ising model. The choice made by the t -th ant for $X(i)$ is denoted as $X(i, t) \in \{0, 1\}$. In typical AS implementations, multiple ants search for the optimal solution simultaneously in each iteration. However, in this model, only one ant conducts the search during each iteration. Since the ants communicate through the pheromones they deposit, this difference is not essential, provided that the pheromones do not evaporate too rapidly. The evaluation of the choice $\{X(i, t)\}, i = 1, \dots, N$ is based on the energy value, denoted as $E(t) = E[\{X(i, t)\}]$. Ant t deposits pheromones on their choices $\{X(i, t)\}$, with the amount of pheromone given by the Boltzmann weight $e^{-E(t)}$. In our previous work, we studied the case where $h(i) = 1, J(i, j) = 0$, and the pheromone value was set to $\frac{-E(t)+N}{2}$ [26]. Here, the term N in $-E(t) + N$ ensures that the pheromone value remains non-negative. The Boltzmann weight pheromone can avoid the negative value of the pheromone, one sees that the approximation in the derivation of SDE needs the restrictions $h(i) \ll 1$ and $J(i, j) \ll 1$.

We assume that the pheromones evaporate and decrease by a factor of $e^{-1/\tau}$ after each iteration, where τ represents the time scale of the pheromone evaporation. The total value of pheromones that remains after ant t 's choices is,

$$S(t) = \sum_{s=1}^t e^{-E(s)-(t-s)/\tau}. \quad (2)$$

The remaining pheromone on the choice $X(k) = x$ is

$$S_x(k, t) = \sum_{s=1}^t e^{-E(s)-(t-s)/\tau} \delta_{X(k,s),x}. \quad (3)$$

Here, $\delta_{x,y}$ represents the Kronecker delta function, which is defined to be 1 if $x = y$ and 0 otherwise.

Ant $t+1$ makes decisions $\{X(k, t+1), k = 1, \dots, N\}$ based on simple probabilistic rules. The information provided by $S_x(k, t)$ gives ant $t+1$ an indirect clue about the choice x . In Bayesian statistics, if $S_1(k, t) > S_0(k, t)$, then the posterior probability that $X(k, t+1) = 1$ exceeds $\frac{1}{2}$; conversely, it is less than $\frac{1}{2}$ if $S_1(k, t) < S_0(k, t)$. We adopt a linear decision function with a positive parameter α as follows:

$$P(X(k, t+1) = 1) = (1 - \alpha) \frac{1}{2} + \alpha \cdot \frac{S_1(k, t)}{S(t)}$$

Here, α determines the response of the choice to the values of the pheromones. $S_1(k, t) = 0$ and $S_1(k, t) = S(t)$ are the absorbing states for $\alpha = 1$, we restrict $\alpha < 1$. When $\alpha = 0$,

$P(X(k, t + 1) = 1) = 1/2$ and the ants choose at random. As α increases, the ants take into account the pheromone in their decisions. In the typical ACO implementation, the decision function adopts a nonlinear form $P(X(k, t + 1) = x) \propto S_x(k, t)^\alpha$. In the binary choice case, the decision under the case $S_1(k, t) \simeq S(t)/2$ is crucial. The above linear form approximates the typical decision function in the crucial case ($S_1(k, t)/S(t) \simeq 1/2$) as,

$$P(X(k, t + 1) = 1) = \frac{S_1(k, t)^\alpha}{S_1(k, t)^\alpha + S_0(k, t)^\alpha} \simeq (1 - \alpha)\frac{1}{2} + \alpha \cdot \frac{S_1(k, t)}{S(t)}$$

We denote the ratio of the remaining pheromones on the choice $X(k) = 1$ as $Z(k, t)$,

$$Z(k, t) \equiv \frac{S_1(k, t)}{S(t)}. \quad (4)$$

The probability of the choice $X(k, t + 1) = 1$ is expressed as

$$P(X(k, t + 1) = 1) = (1 - \alpha)\frac{1}{2} + \alpha Z(k, t) \equiv f(Z(k, t)). \quad (5)$$

Here, we introduce a decision function $f(z)$,

$$f(z) \equiv (1 - \alpha)\frac{1}{2} + \alpha z.$$

The first ant ($t = 1$) makes her choice at random, following a Bernoulli distribution for each k from 1 to N :

$$X(k, 1) \sim \text{Ber}(1/2), \quad k = 1, \dots, N.$$

We denote the history of the process as H_t . Here H_t means all choices $\{X(i, s)\}, i = 1, \dots, N, s = 1, \dots, t$. The conditional expected value of $X(i, t + 1)$ under H_t is

$$\mathbb{E}[X(k, t + 1)|H_t] \equiv E[X(k, t + 1)|\{Z(k, t)\}] = f(Z(k, t)).$$

Likewise, the conditional expected value of $E(t + 1)$ under H_t is estimated as,

$$\begin{aligned} \mathbb{E}[E(t + 1)|H_t] &= - \sum_i h(i)(2f(Z(i, t)) - 1) \\ &\quad - \frac{1}{N - 1} \sum_{i, j, i \neq j} J(i, j)(2f(Z(i, t)) - 1)(2f(Z(j, t)) - 1) \end{aligned}$$

Here, we use the fact that $X(i, t + 1)$ and $X(j, t + 1)$ are conditionally independent. We also introduce the conditional expected value of $\sigma(i, t + 1) = 2X(i, t + 1) - 1$ under H_t , which we call "magnetization" $M(i, t)$, as

$$M(i, t) \equiv \mathbb{E}[2X(k, t + 1) - 1|H_t] = 2(f(Z(i, t))) - 1 = 2\alpha \left(Z(i, t) - \frac{1}{2} \right) \in [-\alpha, \alpha].$$

The conditional expected value of $E(t+1)$ is expressed with $\{M(i, t)\}, i = 1, \dots, N$ as

$$\mathbb{E}[E(t+1)|H_t] = - \sum_i h(i)M(i, t) - \frac{1}{N-1} \sum_{i,j,i \neq j} J(i, j)M(i, t)M(j, t).$$

III. DYNAMICS OF PHEROMONE RATIOS AND STATIONARY DISTRIBUTION

In this section, we investigate the temporal evolution of the system, focusing on the dynamics of pheromone ratios, $Z(k, t) = S_1(k, t)/S(t)$. Starting from the recursive relationship for $S(t)$,

$$S(t+1) = S(t)e^{-1/\tau} + e^{-E(t+1)}, \quad (6)$$

we examine $\Delta S(t) = S(t+1) - S(t)$, especially in the regime where $\tau \gg 1$, leading to

$$\Delta S(t) \approx -\frac{1}{\tau}S(t) + e^{-E(t+1)}.$$

This difference equation illustrates the rate of change of $S(t)$ over time. In the continuous time limit, the differential equation for $S(t)$ is obtained as

$$dS(t) = \left(-\frac{1}{\tau}S(t) + \mathbb{E}[e^{-E(t+1)}|H_t] \right) dt.$$

Here, we neglect the random force term from the variance of $e^{-E(t+1)}$. Assuming the system reaches a stationary state as $t \rightarrow \infty$, $S(t)$ converges to $\tau \mathbb{E}_{st}[e^{-E(t+1)}]$. The subscript $_{st}$ on $\mathbb{E}_{st}[\]$ signifies that the average is taken in the stationary distribution of the process $\{X(i, t)\}$.

The expected value of $S(t)$ in this stationary state, denoted as S_{st} , is given by

$$S_{st} \equiv \tau \mathbb{E}_{st}[e^{-E(t+1)}].$$

A. Stochastic Differential Equation of Pheromone Ratios

To derive the SDEs for $\{Z(k, t)\}$, we analyze the temporal evolution of $\{S_x(k, t)\}$. Decomposing $S_x(k, t+1)$ provides the foundational step:

$$S_x(k, t+1) = S_x(k, t)e^{-1/\tau} + e^{-E(t+1)|_{X(k,t+1)=x}} \delta_{X(k,t+1),x}.$$

We then partition $E(t+1)$ into components based on their dependence on $X(k, t+1)$:

$$\begin{aligned} E(t+1) &= - \sum_{i \neq k} h(i)(2X(i, t+1) - 1) \\ &\quad - \frac{1}{N-1} \sum_{i \neq j, i \neq k, j \neq k} (2X(i, t+1) - 1)(2X(j, t+1) - 1) \\ &\quad - (2X(k, t+1) - 1) \left(h(k) + \frac{1}{N-1} \sum_{l \neq k} 2J(k, l)(2X(l, t+1) - 1) \right). \end{aligned}$$

Introducing the concept of the "effective field" $\hat{h}(k, t+1)$, we define it as follows:

$$\hat{h}(k, t+1) = h(k) + \frac{1}{N-1} \sum_{l \neq k} 2J(k, l)(2X(l, t+1) - 1) = -\frac{1}{2} \frac{\partial E(t+1)}{\partial X(k, t+1)}.$$

For a choice $X(k, t+1) = x$, the energy $E(t+1)$ simplifies to:

$$E(t+1)|_{X(k, t+1)=x} = E(t+1) - 2\hat{h}(k)(x - X(k, t+1)).$$

Assuming a small effective field $\hat{h}(k, t+1)$, which is valid for $h(k) \ll 1$ and $J(k, l) \ll 1$, the approximation of $e^{-E(t+1)}|_{X(k, t+1)=x}$ is:

$$\exp(-E(t+1)|_{X(k, t+1)=x}) \approx \exp(-E(t+1))(1 + 2\hat{h}(k, t+1)(x - X(k, t+1))).$$

Accordingly, $S_x(k, t+1)$ can be reformulated as:

$$S_x(k, t+1) = S_x(k, t)e^{-1/\tau} + e^{-E(t+1)} \left(1 + 2\hat{h}(k, t+1)(x - X(k, t+1)) \right) \delta_{X(k, t+1), x}.$$

Leveraging the above formulation and eq. (6), we deduce that:

$$\begin{aligned} Z(k, t+1) &= \left(1 - \frac{e^{-E(t+1)}}{S(t+1)} \right) Z(k, t) \\ &\quad + \frac{e^{-E(t+1)}}{S(t+1)} \left(1 + 2\hat{h}(k, t+1)(1 - X(k, t+1)) \right) \delta_{X(k, t+1), 1}. \end{aligned}$$

The incremental change in $Z(k, t)$ is thus estimated as:

$$\Delta Z(k, t) \approx \frac{e^{-E(t+1)}}{S(t+1)} \left(\delta_{X(k, t+1), 1} - Z(k, t) + 2\hat{h}(k, t+1)(1 - X(k, t+1))\delta_{X(k, t+1), 1} \right).$$

In the stationary state approximation where $S(t+1) = \tau \mathbb{E}[e^{-E(t+1)}] \approx \tau e^{-E(t+1)}$, we have:

$$\Delta Z(k, t) \simeq \frac{1}{\tau} \left(\delta_{X(k, t+1), 1} - Z(k, t) + 2\hat{h}(k, t+1)(1 - X(k, t+1))\delta_{X(k, t+1), 1} \right).$$

The expected value and the variance of $\Delta Z(k, t)$, conditioned on the history H_t , are approximated as follows:

$$\begin{aligned}\mathbb{E}[\Delta Z(k, t)|H_t] &\simeq \frac{1}{\tau} [f(Z(k, t)) - Z(k, t) \\ &\quad + \mathbb{E} [2\hat{h}(k, t+1)|H_t] (1 - f(Z(k, t)))f(Z(k, t))], \\ \mathbb{V}[\Delta Z(k, t)|H_t] &\simeq \frac{1}{\tau^2} \mathbb{V}[\delta_{X(k, t+1), 1}|H_t] = \frac{1}{\tau^2} f(Z(k, t))(1 - f(Z(k, t))).\end{aligned}$$

Here, we approximate the expected value of the product of the random variables as the product of the expected values of the random variables. In addition, we neglect the variance of the third term of $\Delta Z(k, t)$, which is valid when $\hat{h}(k, t+1) \ll 1$.

The conditional expected value of the effective field $\hat{h}(k, t+1)$ under H_t is,

$$\begin{aligned}\mathbb{E}[\hat{h}(k, t+1)|H_t] &= h(k) + \frac{2}{N-1} \sum_{l \neq k} J(k, l) (2f(Z(l, t)) - 1) \\ &= h(k) + \frac{2}{N-1} \sum_{l \neq k} J(k, l) 2\alpha \left(Z(l, t) - \frac{1}{2} \right) \\ &\equiv \tilde{h}(k, t).\end{aligned}$$

We note that the conditional expected value of $\hat{h}(k, t+1)$ under H_t is a function of H_t . Given the decision function $f(z) = (1-\alpha)\frac{1}{2} + \alpha(z - \frac{1}{2})$, and its complement $1 - f(z) = \frac{1}{2} - \alpha(z - \frac{1}{2})$, $f(z)(1 - f(z)) = \frac{1}{4} - \alpha^2(z - 1/2)^2$. We have:

$$\begin{aligned}\mathbb{E}[\Delta Z(k, t)|H_t] &\simeq \frac{1}{\tau} \left[-(1-\alpha) \left(Z(k, t) - \frac{1}{2} \right) + 2\tilde{h}(k, t) \left(\frac{1}{4} - \alpha^2 \left(Z(k, t) - \frac{1}{2} \right)^2 \right) \right], \\ \mathbb{V}[\Delta Z(k, t)|H_t] &\simeq \frac{1}{\tau^2} \left(\frac{1}{4} - \alpha^2 \left(Z(k, t) - \frac{1}{2} \right)^2 \right).\end{aligned}\tag{7}$$

The SDEs describing the dynamics of $\{Z(k, t)\}$ are given by:

$$dZ(k, t) = \mathbb{E}[\Delta Z(k, t)|H_t]dt + \sqrt{\mathbb{V}[\Delta Z(k, t)|H_t]}dW(k, t).\tag{8}$$

where $\vec{W}(t) = \{W(k, t)\}, k = 1, \dots, N$, represents an independent and identically distributed Wiener process, and $d\vec{W}(t)$ follows a $N_N(0, Idt)$ distribution. We denote d -dimensional normal distribution with expectation $\vec{\mu}$ and variance Σ as $N_d(\vec{\mu}, \Sigma)$.

In multiplying eq. (8) by 2α , we obtain the SDEs for $\{M(k, t)\}$ as follows:

$$\begin{aligned}dM(k, t) &= \frac{1}{\tau} \left(-(1-\alpha)M(k, t) + \alpha\tilde{h}(k, t)(1 - M(k, t)^2) \right) dt \\ &\quad + \left(\frac{\alpha}{\tau} \right) \sqrt{1 - M(k, t)^2} dW(k, t), \quad M(k, t) \in [-\alpha, \alpha].\end{aligned}\tag{9}$$

The Fokker-Planck equation for the joint PDF of $\vec{M}(t) = (M(1, t), \dots, M(N, t))$ is [27],

$$\begin{aligned} \partial_t p(\vec{m}, t) &= -\frac{1}{\tau} \sum_k \partial_{m_k} \left(-(1 - \alpha)m_k + \alpha \tilde{h}_k (1 - m_k^2) \right) p(\vec{m}, t) \\ &\quad + \frac{1}{2} \left(\frac{\alpha}{\tau} \right)^2 \sum_k \partial_{m_k}^2 (1 - m_k^2) p(\vec{m}, t), \\ \tilde{h}_k &\equiv h(k) + \frac{2}{N-1} \sum_{l \neq k} J(k, l) m_l. \end{aligned} \tag{10}$$

B. Stationary Distribution of Pheromone Ratios

We derive the stationary solution of the Fokker-Planck equation (10). We define $A(m|h)$ and $B(m)$ as follows:

$$\begin{aligned} A(m|h) &= \frac{1}{\tau} \left(-(1 - \alpha)m + \alpha h (1 - m^2) \right), \\ B(m) &= \frac{\alpha}{\tau} \sqrt{1 - m^2}. \end{aligned}$$

The Fokker-Planck equation (10) can be expressed as:

$$\partial_t p(\vec{m}, t) = \sum_k \left\{ -\partial_{m_k} A(m_k | \tilde{h}_k) + \frac{1}{2} \partial_{m_k}^2 B^2(m_k) \right\} p(\vec{m}, t).$$

We define J_k as:

$$J_k \equiv \left\{ A(m_k | \tilde{h}_k) - \frac{1}{2} \partial_{m_k} B^2(m_k) \right\} p(\vec{m}, t).$$

Thus, the Fokker-Planck equation simplifies to:

$$\partial_t p(\vec{m}, t) = - \sum_k \partial_{m_k} J_k.$$

To obtain the stationary solution where $\partial_t p(\vec{m}, t) = 0$, we solve for $J_k = 0$ [27]. We apply the reflecting boundary condition:

$$J_k(m_k = \pm \alpha) = 0.$$

From $J_k = 0$, we obtain:

$$\left\{ A(m_k | \tilde{h}_k) - \frac{1}{2} \partial_{m_k} B^2(m_k) \right\} p_{st}(\vec{m}) = \left\{ \frac{1}{2} B^2(m_k) \right\} \partial_{m_k} p_{st}(\vec{m}).$$

We define Z_k as:

$$Z_k \equiv \frac{A(m_k | \tilde{h}_k) - \frac{1}{2} \partial_{m_k} B^2(m_k)}{\frac{1}{2} B^2(m_k)} = \frac{2A(m_k | \tilde{h}_k)}{B^2(m_k)} - \partial_{m_k} \log B^2(m_k).$$

It follows that:

$$\partial_{m_k} \log p_{st}(\vec{m}) = Z_k.$$

The potential $\phi(\vec{m})$ for the potential solution $p_{st}(\vec{m}) \propto e^{-\phi(\vec{m})}$ satisfies:

$$\partial_{m_k} \phi(\vec{m}) = -Z_k.$$

The existence of $\phi(\vec{m})$ is guaranteed by the condition [27]:

$$\partial_{m_l} Z_k = 2 \left(\frac{\tau}{\alpha} \right) \frac{2}{N-1} J(k, l) = 2 \left(\frac{\tau}{\alpha} \right) \frac{2}{N-1} J(l, k) = \partial_{m_k} Z_l.$$

The potential $\phi(\vec{m})$ is given by:

$$\begin{aligned} \phi(\vec{m}) = & - \int^{\vec{m}} \vec{Z} d\vec{m} = - \left(\left(\frac{\tau}{\alpha^2} \right) (1 - \alpha) - 1 \right) \sum_k \log(1 - m_k^2) \\ & - 2 \left(\frac{\tau}{\alpha} \right) \sum_k \left\{ h(k) + \frac{1}{N-1} \sum_{l \neq k} J(k, l) m_l \right\} m_k. \end{aligned}$$

The joint PDF of the stationary state $p_{st}(\vec{m})$ is given as:

$$\begin{aligned} p_{st}(\vec{m}) \propto & \exp \left(\sum_k \left\{ \frac{1}{2} a(\alpha) \log(1 - m_k^2) + 2 \left(\frac{\tau}{\alpha} \right) \left(h(k) m_k + \frac{1}{N-1} \sum_{l \neq k} J(k, l) m_k m_l \right) \right\} \right), \\ a(\alpha) \equiv & 2 \left(\left(\frac{\tau}{\alpha^2} \right) (1 - \alpha) - 1 \right). \end{aligned} \quad (11)$$

We assume the stability of the system and that $\vec{m} = \vec{0}$ should be the unique mode for $J(k, l) = h(k) = 0$. We restrict α so that the coefficient $a(\alpha)$ of $\log(1 - m_k^2)$ is positive. We set the upper bound of α as $1 - \frac{1}{\tau} < 1$ and ensure that $a(1 - \frac{1}{\tau}) = 2(1/\alpha^2 - 1) > 0$.

In the derivation of the SDEs, we assume that $\tau \gg 1$. We neglect the last term -1 in $a(\alpha)$, which is valid for $\tau \gg 1$ and $1 - \alpha \gg \frac{1}{\tau}$. We introduce the energy term of the Ising model in the stationary state as a function of \vec{m} as:

$$E_{\text{Ising}}(\vec{m}) = - \sum_k h(k) m_k - \frac{1}{N-1} \sum_{k, l, k \neq l} J(k, l) m_k m_l.$$

We also introduce the entropy energy of the AS as:

$$E_{\text{AS}}(\vec{m}) = - \sum_k \log(1 - m_k^2).$$

The stationary distribution $p_{st}(\vec{m})$ is expressed as:

$$p_{st}(\vec{m}) \propto \exp \left(- \left(\frac{2\tau}{\alpha^2} \right) \left[(1 - \alpha) E_{\text{AS}}(\vec{m}) + \alpha E_{\text{Ising}}(\vec{m}) \right] \right). \quad (12)$$

The terms in the square bracket in the right-hand side of eq. (12) define the "free energy" of the AS. When $\alpha \ll 1$, the entropy energy term $E_{\text{AS}}(\vec{m})$ dominates the free energy. As $m_k \in [-\alpha, \alpha]$, the modes of $p_{st}(\vec{m})$ should exist near $\vec{0}$. A small α initially enables the system to avoid premature convergence by maintaining a broad exploration space, which is vital for escaping local minima. As α increases, the energy term $E_{\text{Ising}}(\vec{m})$ begins to dominate the free energy. The exploration space is restricted to a local minimum of $E_{\text{Ising}}(\vec{m})$, allowing for intensive exploration and exploitation around the promising regions. When $\alpha \approx 1 - \frac{1}{\tau} \approx 1$, $\tau \gg 1$, the entropy energy term disappears and the stationary distribution of \vec{m} is governed by the Boltzmann weight $\exp(-(2\tau/\alpha)E_{\text{Ising}}(\vec{m}))$. The inverse temperature β of the AS is given by:

$$\beta = 2\tau/\alpha.$$

The range of $m_k \in [-(1 - 1/\tau), 1 - 1/\tau]$ is wide and the mode of $p_{st}(\vec{m})$ corresponds to the local minimum of $E_{\text{Ising}}(\vec{m})$.

In terms of Bayesian statistics, the AS provides $\exp(-(\frac{2\tau}{\alpha^2})(1 - \alpha)E_{\text{AS}}(\vec{m}))$, $-\alpha \leq m_k \leq \alpha$ as a prior. Multiplied by the likelihood of \vec{m} , $\exp(-\beta E_{\text{Ising}}(\vec{m}))$, the posterior gives $p_{st}(\vec{m})$. In order to obtain the global minimum of $E_{\text{Ising}}(\vec{m})$ in the α -annealing process, the inverse temperature β should be increased with the increase of α .

The essential difference between Simulated Annealing (SA) and α -annealing of ACO is the path of the annealing process. In α -annealing, the system connects the unique and trivial global minimum of the entropy energy $E_{\text{AS}}(\vec{m})$ and the global minimum of the Ising energy $E_{\text{Ising}}(\vec{m})$. This feature reminds us of the similarity between α -annealing and quantum annealing [24]. Additionally, in α -annealing, the range of the solution \vec{m}_* should be restricted as $m_{*,k} \in [-\alpha, \alpha]$. With these two factors, the α -annealing process addresses the problem of exploration-exploitation trade-off.

The modes \vec{m}_* of $p_{st}(\vec{m})$ satisfy the following relation:

$$a(\alpha) \frac{m_{k*}}{1 - m_{k*}^2} = 2 \left(\frac{\tau}{\alpha} \right) \left(h(k) + \frac{2}{N-1} \sum_{l \neq k} J(k, l) m_{l*} \right).$$

This equation corresponds with the TAP equation in spin-glass theory [28]. The fluctuation of \vec{m} around \vec{m}_* can be approximated by a Gaussian distribution as:

$$p_{st}(\Delta\vec{m}) \propto \exp\left(-\frac{1}{2} \Delta\vec{m}^T \Sigma^{-1} \Delta\vec{m}\right),$$

where $\Sigma_{k,l}^{-1}$ is given by:

$$\Sigma_{k,l}^{-1} = \begin{cases} -4 \left(\frac{\tau}{\alpha}\right) \frac{J(k,l)}{N-1} & k \neq l \\ a(\alpha) \frac{(1+m_{k*}^2)}{(1-m_{k*}^2)^2} & k = l \end{cases}$$

In the Gaussian approximation, \vec{m} obeys a multi-dimensional normal distribution as:

$$\vec{m} \sim N_N(\vec{m}_*, \Sigma).$$

In the stationary distribution $p_{st}(\vec{m})$, the local behavior around each mode \vec{m}_* approximates a normal distribution. When there are multiple modes, $\{\vec{m}_*\}$, the relative probabilities of the system being near any particular mode are roughly determined by $p_{st}(\vec{m}_*)$. Consequently, the overall distribution of \vec{m} can be characterized as a mixture of normal distributions. Each component of this mixture corresponds to a normal distribution centered at a mode \vec{m}_* , with the mixing weights given by the values of $p_{st}(\vec{m}_*)$ at these modes. This formulation captures the system's tendencies towards different stable states under varying conditions, reflecting the multimodal nature of the landscape defined by the stationary distribution.

IV. HOMOGENEOUS FULLY CONNECTED ISING MODEL CASE

We study the stationary distribution $p_{st}(\vec{m})$ for the homogeneous fully connected Ising model. We adopt $J(k,l) = J$ and $h(k) = h$. The mode \vec{m}_* is homogeneous, so we write $\vec{m}_* = m_* \vec{1}$, where $\vec{1}$ is an N -dimensional vector with all components equal to 1. We define b as:

$$b \equiv -4 \left(\frac{\tau}{\alpha}\right) \frac{1}{N-1} J.$$

m_* satisfies the following relation:

$$(a(\alpha) + (N-1)b)m_* - (N-1)bm_*^3 - 2 \left(\frac{\tau}{\alpha}\right) h(1 - m_*^2) = 0. \quad (13)$$

This is a cubic equation with at most three real solutions.

A. $h = 0$ Case

When $h = 0$, m_* satisfies:

$$m_*((a(\alpha) + (N-1)b) - (N-1)bm_*^2) = 0. \quad (14)$$

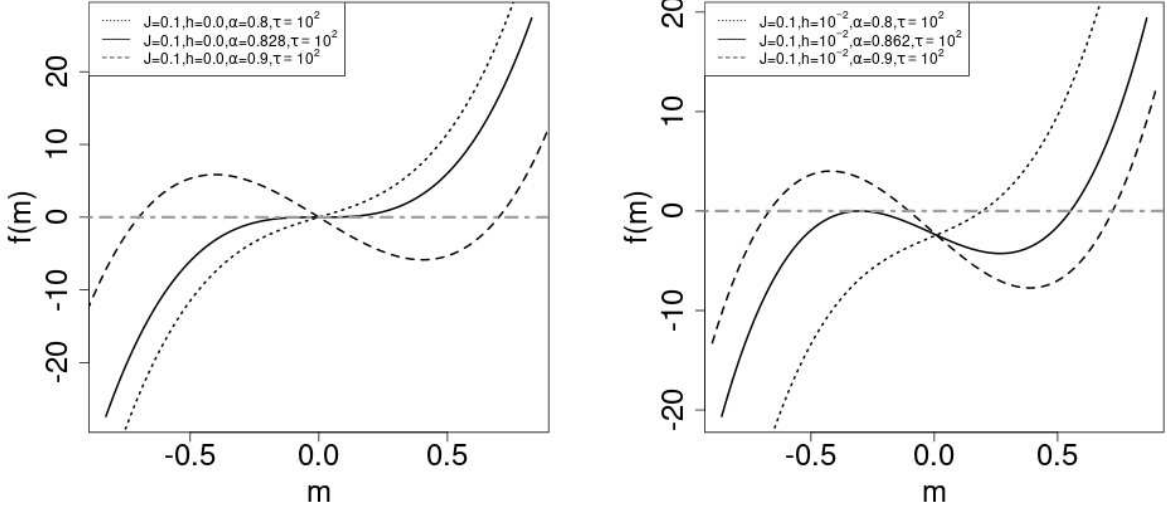


FIG. 1. Plot of cubic equation (13) vs. m . $J = 0.1, h = 0.0$ (Left) and $J = 0.1, h = 0.01$ (Right). $\alpha = 0.8$ (dotted), $\alpha = \alpha_c(h)$ (solid), and $\alpha = 0.9$ (broken).

In addition to the solution $m_* = 0$, when $a(\alpha) + (N - 1)b < 0$, there appear two other real solutions. At $\alpha = \alpha_c$, $a(\alpha_c) + (N - 1)b = 0$ holds. α_c is given as:

$$\alpha_c = \frac{\sqrt{\tau^2(2J + 1)^2 + 4\tau} - \tau(2J + 1)}{2} \simeq \frac{1}{1 + 2J}.$$

The left figure in Figure 1 shows the plot of the cubic equation (13) vs. m for $J = 0.1, h = 0.0$. $\alpha_c = 0.82765$, and we choose $\alpha = 0.8, \alpha_c$, and 0.9 .

For $\alpha \leq \alpha_c$, $m_* = 0$ is the unique solution. Above α_c , two other solutions appear: z_- and z_+ . They are given as:

$$z_+ = -z_- = \sqrt{\frac{a(\alpha) + (N - 1)b}{(N - 1)b}} \propto (\alpha - \alpha_c)^{1/2}.$$

We summarize the results as:

$$m_* = \begin{cases} 0 & \alpha \leq \alpha_c \\ 0, \pm \sqrt{\frac{a(\alpha) + (N - 1)b}{(N - 1)b}} & \alpha > \alpha_c \end{cases}$$

For $\alpha \leq \alpha_c$, $p_{st}(\vec{m})$ becomes maximal at $\vec{m}_* = \vec{0}$. For $\alpha > \alpha_c$, $p_{st}(\vec{m})$ becomes maximal at z_+ and z_- . At $\vec{m} = \vec{0}$, $p_{st}(\vec{m})$ becomes minimal.

B. $h > 0$ Case

When $h > 0$, there is also a threshold value $\alpha_c(h)$ for α . For $\alpha < \alpha_c(h)$, there is a positive real solution, z_+ , where $p_{st}(\vec{m})$ becomes maximal. At $\alpha = \alpha_c(h)$, there are two real solutions, $z_t < z_+$. The smaller solution z_t is a multiple root of eq. (13), and $p_{st}(\vec{m})$ is not maximal. At z_+ , $p_{st}(\vec{m})$ becomes maximal. For $\alpha > \alpha_c$, there are three real solutions: $z_- < z_u < z_+$. We denote the smallest and the largest solutions as z_- and z_+ , respectively. $p_{st}(\vec{m})$ becomes maximal at these solutions. At the middle solution z_u , $p_{st}(\vec{m})$ is minimal.

C. $\alpha_c(h)$ and m_*

We solve eq. (13) numerically to obtain $\alpha_c(h)$. We also obtain the real solutions m_* vs. α . Figure 2 summarizes the results.

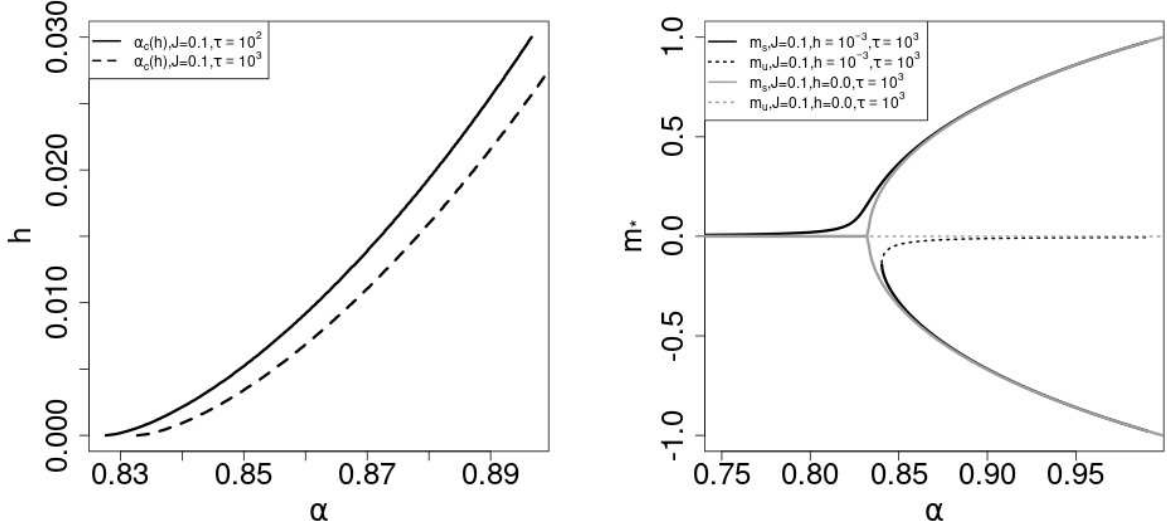


FIG. 2. h vs. $\alpha_c(h)$ (Left) and m_* vs. α (Right). In the left figure, we adopt $J = 0.1, \tau = 10^2$ (solid line) and $J = 0.1, \tau = 10^3$ (broken line). In the right figure, we adopt $J = 0.1, h = 0.0$ (gray) and $J = 0.1, h = 10^{-3}$ (black). The solid lines show the solutions where $p_{st}(\vec{m})$ becomes maximal, and the dotted lines show the solutions where $p_{st}(\vec{m})$ becomes minimal.

D. Correlation of \vec{M}

The inverse of the covariance Σ^{-1} is given as:

$$\Sigma_{k,l}^{-1} = \begin{cases} b & k \neq l \\ a' \equiv a(\alpha) \frac{(1+m_*^2)}{(1-m_*^2)^2} & k = l \end{cases}$$

The inverse matrix of $(a' - b)I + bJ$, where I is the identity matrix and J is the matrix with all components equal to 1, is given as:

$$((a' - b)I + bJ)^{-1} = \frac{1}{a' - b}I - \frac{b}{a' + (N - 1)b} \cdot \frac{1}{a' - b}J.$$

Using this result, we obtain Σ :

$$\Sigma_{k,l} = \begin{cases} \frac{1}{a' - b} \cdot \frac{-b}{a' + (N - 1)b} & k \neq l \\ \frac{1}{a' - b} \left(1 + \frac{-b}{a' + (N - 1)b} \right) & k = l \end{cases}$$

The correlation coefficient between M_i and M_j is:

$$\text{Corr.}(M_i, M_j) = \frac{\Sigma_{i,j}}{\sqrt{\Sigma_{i,i}\Sigma_{j,j}}} = \frac{-b}{a' + (N - 2)b}.$$

In the case $h = 0$, at $\alpha = \alpha_c(h = 0)$, $m_* = 0$ and $a' = a$. $a(\alpha_c) + (N - 1)b = 0$ holds, and $\text{Corr.}(M_i, M_j) = 1$.

E. Marginal pdf of M_i

In the Gaussian approximation, for $\alpha < \alpha_c(h)$, the marginal distribution of M_i around the mode m_* is given as:

$$p_{st}(m_i) \propto \exp\left(-\frac{1}{2\Sigma_{i,i}}(m_i - m_*)^2\right), \quad m_i \in [-\alpha, \alpha],$$

$$\Sigma_{i,i} = \frac{1}{a' - b} \left(1 + \frac{-b}{a' + (N - 1)b} \right), \quad a' = a(\alpha) \frac{(1 + m_*^2)}{(1 - m_*^2)^2}.$$

Here, m_* is the unique solution of eq. (13).

For $h = 0$, at the critical point $\alpha = \alpha_c(0)$, $\Sigma_{i,i}$ diverges and the Gaussian approximation breaks down. We cannot neglect the higher order terms in $\log(1 - m_i^2)$, and $p_{st}(m)$ is given as:

$$p_{st}(m_i) \propto \exp\left(-\frac{1}{2\Sigma_{i,i}}(m_i - m_*)^2\right) \cdot \exp\left(\frac{1}{2}a(\alpha)\{\log(1 - m_i^2) + m_i^2\}\right).$$

At the critical point $\alpha = \alpha_c(0)$, the first term on the right-hand side of $p_t(m_i)$ becomes 1, and the second term describes the PDF.

Above α_c , $p_{st}(\vec{m})$ has two modes at \vec{m}_+ and \vec{m}_- , where $\vec{m}_+ = m_+\vec{1}$ and $\vec{m}_- = m_-\vec{1}$. We denote the relative probabilities for the two modes m_+ and m_- as p_+ and p_- , respectively. For $h = 0$, $p_+ = p_- = 1/2$. $p_{st}(m_i)$ is the mixture of the two normal distributions approximately:

$$p_{st}(m_i) \propto p_+ \exp\left(-\frac{1}{2\Sigma_{i,i}(+)}(m_i - m_+)^2\right) + p_- \exp\left(-\frac{1}{2\Sigma_{i,i}(-)}(m_i - m_-)^2\right).$$

Here, $\Sigma_{i,i}(+)$ and $\Sigma_{i,i}(-)$ are estimated using m_+ and m_- , respectively. For $h > 0$, we need to estimate p_+ and p_- using the relation:

$$\frac{p_+}{p_-} = \frac{p_{st}(\vec{m}_+)}{p_{st}(\vec{m}_-)} \simeq \exp\left(-\frac{2\tau}{\alpha}\{E_{Ising}(\vec{m}_+) - E_{Ising}(\vec{m}_-)\}\right).$$

V. NUMERICAL STUDY OF α -ANNEALING

We have conducted numerical simulations to validate the theoretical predictions associated with α -annealing in the homogeneous fully connected Ising model. $\{M(i, t) = 2\alpha(Z(i, t) - 1/2)\}$ were sampled according to the following annealing schedule:

$$\alpha(t) = \frac{t}{T}, \quad \alpha(t) < 1 - \frac{1}{\tau}, \quad t = 0, 1, \dots,$$

We set $T = 10^6$ and $T = 10^4$ and refer to them as "slow" and "fast" annealing, respectively. In the annealing process, the increment of α is given by $\Delta\alpha = 1/T$. We conducted $S = 1000$ trials for each schedule. $M(i, t, s)$ represents the magnetization at time t for $X(i)$ during trial s .

We considered a system size of $N = 100$ spins. We set the parameters as $h = 10^{-3}$, $J = 10^{-1}$, and $\tau \in \{10^2, 10^3\}$. In addition, when studying the stationary distribution of $\{M(i, t)\}$ for specific J , h , and α , we adopted the slow annealing schedule with fixed J and h . If $\alpha(t)$ reaches a specific value, we sampled $\{M(i, t)\}$ only once in order to ensure the independence of the sampling process. We repeated the process 5×10^3 times and studied the PDF of $\{M(i, t, s)\}$, $s = 1, \dots, 5 \times 10^3$. The sample size of $\{M(i, t)\}$ is $5 \times 10^3 \times N = 5 \times 10^5$.

When comparing the performance of α -annealing with simulated annealing (SA), we performed SA with the conventional Metropolis-Hastings update algorithm. For τ , we set

the final inverse temperature as $\beta = 2\tau$ and the increment of β after each Monte Carlo step is set as:

$$\Delta\beta = \frac{2\tau}{T}.$$

We have done the sampling process 10^4 times and estimated the success probability to find the ground state of the model.

The conditions for comparison of the two algorithms were kept identical. In ACO, every ant chose $X(i), i = 1, \dots, N$ and the number of ants was about 10^6 under the slow annealing schedule. While in SA, the final inverse temperature β was reached after 10^6 Monte Carlo steps (MCS). In one MCS, the number of trials for the spin update is N .

A. Stationary distribution of $M(i, t)$

We studied the stationary distribution of $M(i, t)$. Figure 3 shows the results for the PDF $p(m)$ of $M(i, t)$. We adopted $J = 0.1$, $h = 10^{-3}$, and $\tau = 10^2$ and $\tau = 10^3$. There are three figures for $\alpha = 0.8$, $\alpha_c(h)$, and $\alpha = 0.9$, respectively. The fourth figure shows the plot of the cubic equation (13) versus m for $J = 0.1$, $h = 10^{-3}$, and $\tau = 10^2$. $\alpha_c = 0.83515$ for $J = 0.1, h = 10^{-3}, \tau = 10^2$ and we chose $\alpha = 0.8, \alpha_c$, and 0.9 .

As one can see clearly, for $\alpha = 0.8 < \alpha_c(h)$, there is a unique mode for $p(m)$. The variance of the PDF is smaller for larger τ . The vertical broken line shows the position of the mode m_* in the theory, where a discrepancy is observed. For $\alpha = 0.9 > \alpha_c(h)$, there are two modes and the values of the modes are almost consistent with the theoretical ones. At $\alpha = \alpha_c(h)$, for $\tau = 10^2$, the PDF has two modes, which is consistent with the plot of the cubic equation in the last figure (Lower Right). The profile of the cubic equation is almost flat near z_t . The probability current is positive for $z_t < z < z_+$, indicating that the lower mode should disappear finally. However, the stability of the mode of $p_{st}(m)$ at $m = m_t$ is a very subtle problem. For $\tau = 10^3$, the profile of the PDF is not smooth and the result suggests that the equilibration is not enough for $\tau = 10^3$.

B. The comparison of α -annealing with simulated annealing

We studied the performance of α -annealing in ACO. We determined $\{X(i, t)\}$ from $\{M(i, t)\}$ by $X(i, t) = \theta(M(i, t))$, where $\theta(x)$ is the step function, i.e., $\theta(x) = 1$ for $x > 0$

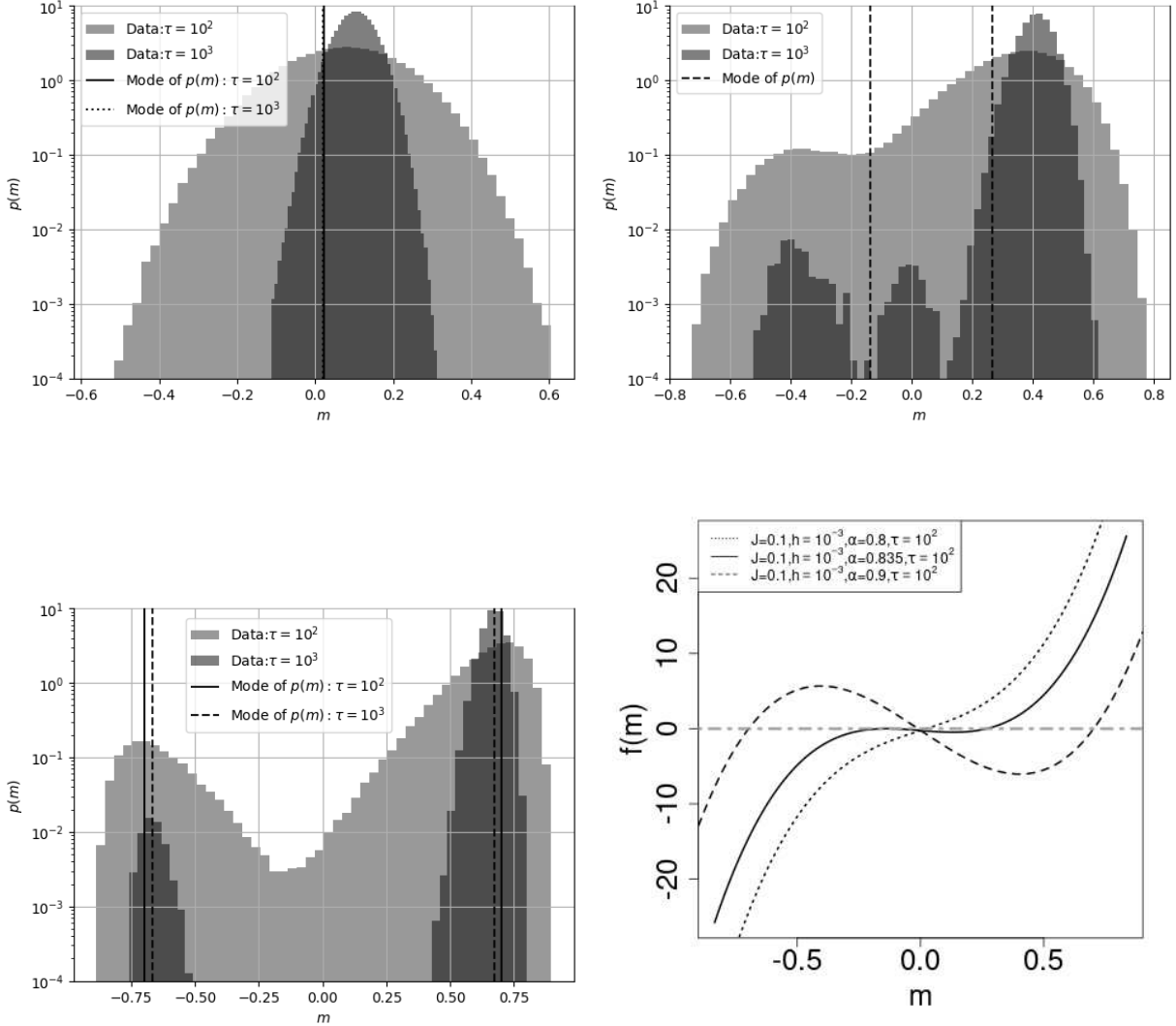


FIG. 3. Plot of $p(m)$ for $\alpha = 0.8$ (Upper Left), $\alpha_c(h = 0.001)$ (Upper Right), and 0.9 (Lower Left), and plot of cubic equation (13) vs. m (Lower Right) for $J = 0.1$, $h = 10^{-3}$. In the figures of $p(m)$, the gray ones show $p(m)$ for $\tau = 10^2$ and the black ones show $p(m)$ for $\tau = 10^3$. The plots of the cubic equation correspond to the cases in the three figures of $p(m)$ for $\tau = 10^2$.

and $\theta(x) = 0$ for $x \leq 0$. The ACO system finds the ground state of the homogeneous fully connected Ising model, $\{\forall i, X(i) = 1\}$, if $\{\forall i, M(i, t) > 0\}$. We counted the number of samples where $\{\forall i, M(i, t) > 0\}$ holds among 10^3 samples and estimated the success probability. Figure 4 plots the success probability versus α . For $\tau = 10^2$ and $\tau = 10^3$, there are two results for both fast and slow annealing processes, respectively.

In the fast annealing cases, the success probability is almost zero and the system cannot

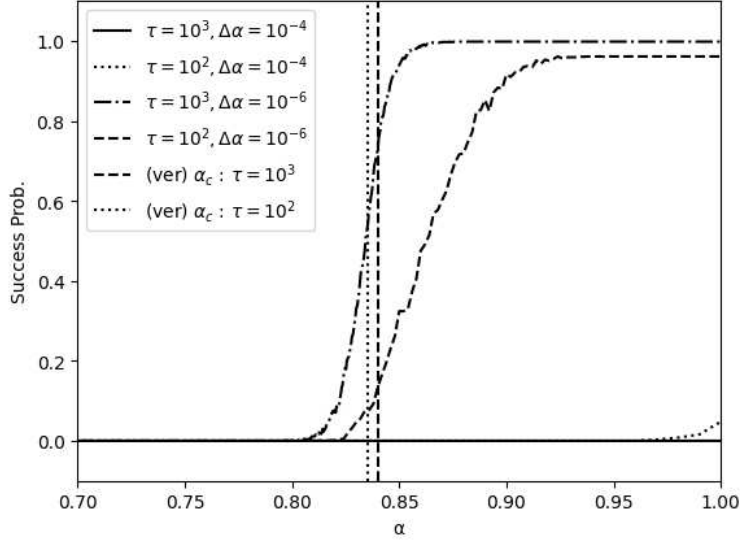


FIG. 4. Plot of α versus the success probabilities to find the ground state of the Ising model. Fast annealing processes ($T = 10^4, \Delta\alpha = 10^{-4}$) for $\tau = 10^2$ (solid line) and $\tau = 10^3$ (dotted line), and slow annealing processes ($T = 10^6, \Delta\alpha = 10^{-6}$) for $\tau = 10^2$ (broken line) and $\tau = 10^3$ (chain line). The vertical lines show α_c for $J = 0.1$ and $h = 10^{-3}$.

find the ground state. In the slow annealing cases, the success probability begins to increase near α_c . It reaches 998/1000(961/1000) at $\alpha = 1 - 1/\tau$ for $\tau = 10^3(10^2)$. The success probability in SA is 0.6024 for 10^4 trials. The results show that the performance of α -annealed ACO is much better than that of SA.

When $h = 0$, the critical value of β is $\beta_c = 1/J = 10$ for $J = 0.1$ in SA. $\beta(t) = (2 \times \tau/T)t$ reaches β_c at $t = 5 \times 10^3$ for $\tau = 10^3, T = 10^6$. It is a rather fast annealing process and SA cannot find the ground state with high success probability. When $\beta(t) \simeq \beta_c$, the correlation among the spin variables becomes strong and it becomes random whether $\{\forall i, X(i, t) = 1\}$ or $\{\forall i, X(i, t) = 0\}$.

As seen in Figure 2, there is a continuous curve that connects the trivial solution $\{\forall i, M(i, t) \simeq 0\}$ for $\alpha \simeq 0$ with the correct solution $\{\forall i, M(i, t) > 0\}$ at $\alpha = 1 - 1/\tau$. By slow annealing of α , the PDF $p(m)$ is concentrated around m_+ and the mode of $p(m)$ is brought along the curve. When $\alpha(t)$ passes α_c , the gap between m_+ and m_t is large compared with the width of $p(m)$ for $\tau = 10^3$. At $\alpha = 1 - 1/\tau$, it is possible to keep the PDF around $m_+ \simeq 1$ for $\tau = 10^3$. The system can find the ground state with high success

probability. For $\tau = 10^2$, the width of $p(m)$ is wide and jumps from m_+ to m_t occur. As a result, the success probability becomes small. In fast annealing cases ($T = 10^4, \Delta\alpha = 10^{-4}$), the equilibration of $M(i, t)$ is not sufficient and it is difficult to align all $M(i, t)$. The success probability is much lower than the result of SA.

VI. CONCLUSION

This paper has explored the effectiveness of α -annealing within the Ant Colony Optimization (ACO) framework, particularly in seeking the ground state of the infinite-range Ising model. Our analysis, underpinned by Stochastic Differential Equations (SDEs), revealed that the joint probability density function (PDF) of the pheromone ratios is composed of two factors: entropy from the Ant System (AS) and energy from the Ising model. The parameter α plays a crucial role in balancing these factors, providing a mechanism to adjust the system's focus from broad exploratory searches to more targeted exploitative searches as α increases.

We demonstrated that a smaller α initially enables the system to avoid premature convergence by maintaining a broad exploration space, which is vital for escaping local minima. As α increases, the exploration space narrows, allowing for intensive exploration around promising regions previously identified. This dynamic is akin to the principles observed in quantum annealing, making α -annealing a potent strategy for navigating complex optimization landscapes.

Moreover, the careful management of α and τ —particularly the rate of pheromone evaporation—is shown to be essential for the system's ability to equilibrate and ultimately find the global minimum. Similar to temperature control in simulated annealing, α and τ control in α -annealing ensures that the system can effectively balance between exploration and exploitation, adapting to the complexity of the optimization challenges.

In conclusion, α -annealing emerges as a sophisticated and efficient strategy for enhancing ACO's performance in complex optimization scenarios. This study not only underscores the potential of α -annealing as a viable alternative to traditional optimization techniques like simulated annealing but also highlights its unique ability to manage and manipulate exploration spaces dynamically. Future work will explore further applications of α -annealing across different types of optimization problems, seeking to generalize these findings and refine

the approach for broader practical implementation.

Acknowledgements.

This work was supported by JPSJ KAKENHI [Grant No. 22K03445].

- [1] M. Dorigo, *Optimization, learning and Natural algorithms*, Ph.D. thesis, Poltecnico di Milan (1992).
- [2] M. Dorigo and L. M. Gambardella, Ant colonies for the travelling salesman problem, *Biosystems* **43**, 73 (1997).
- [3] J. Deneubourg, S. Aron, S. Goss, and J. Pasteels, Error, communication and learning in ant societies, *European Journal of Operational Research* **30**, 168 (1987), modelling Complex Systems I.
- [4] J. Pasteels, J.-L. Deneubourg, and S. Goss, Transmission and amplification of information in a changing environment: The case of insect societies, *Law of Nature and Human Conduct* , 129 (1987).
- [5] J. Pasteels, J. Deneubourg, and C. Detrain, *Information processing in social insects* (Birkhauser Verlag, Basel, 2007).
- [6] S. Camazine and J. Deneubourg, *Self-organization in biological systems* (Princeton University Press, NJ, 2001).
- [7] A. Kirman, Ants, rationality and recruitment, *Q. J. Econ.* **108**, 137 (1993).
- [8] M. Hisakado and S. Mori, Information cascade, kirman’s ant colony model, and kinetic ising model, *Physica A: Statistical Mechanics and its Applications* **417**, 63 (2015).
- [9] O. Cordón, F. Herrera, and T. Stützle, A review on the ant colony optimization metaheuristic: basis, models and new trends., *Mathware and Soft Computing* **9**, 141 (2002).
- [10] M. Dorigo and T. Stützle, Ant colony optimization: Overview and recent advances, in *Handbook of Metaheuristics*, edited by M. Gendreau and J.-Y. Potvin (Springer US, Boston, MA, 2010) pp. 227–263.
- [11] W. Li, L. Xia, Y. Huang, and S. Mahmoodi, An ant colony optimization algorithm with adaptive greedy strategy to optimize path problems,

- Journal of Ambient Intelligence and Humanized Computing **13**, 1557 (2022).
- [12] K. Tang, X.-F. Wei, Y.-H. Jiang, Z.-W. Chen, and L. Yang, An adaptive ant colony optimization for solving large-scale traveling salesman problem, *Mathematics* **11**, 10.3390/math11214439 (2023).
- [13] N. Meuleau and M. Dorigo, Ant Colony Optimization and Stochastic Gradient Descent, *Artificial Life* **8**, 103 (2002).
- [14] T. Stutzle and M. Dorigo, A short convergence proof for a class of ant colony optimization algorithms, *IEEE Transactions on Evolutionary Computation* **6**, 358 (2002).
- [15] W. J. Gutjahr, Aco algorithms with guaranteed convergence to the optimal solution, *Information Processing Letters* **82**, 145 (2002).
- [16] W. J. Gutjahr, A converging aco algorithm for stochastic combinatorial optimization, in *Stochastic Algorithms: Foundations and Applications*, edited by A. Albrecht and K. Steinhöfel (Springer Berlin Heidelberg, Berlin, Heidelberg, 2003) pp. 10–25.
- [17] Y. Nakamichi and T. Arita, Diversity control in ant colony optimization, *Artificial Life and Robotics* **7**, 198 (2004).
- [18] M. Randall and E. Tonkes, Intensification and diversification strategies in ant colony system, *Complexity International* **9**, 1 (2002).
- [19] B. Meyer, On the convergence behaviour of ant colony search, *Complexity International* **12**, 1 (2008).
- [20] B. Meyer, On the convergence behaviour of ant colony search, in *Proceedings of the 7th Asia-Pacific Complex Systems Conference (COMPLEX 2004)*, edited by R. Stonier, Q. Han, and W. Li (Central Queensland University, Australia, 2004) pp. 153 – 167, Asia-Pacific Complex Systems Conference (COMPLEX) ; Conference date: 01-01-2004.
- [21] B. Meyer, A tale of two wells: Noise-induced adaptiveness in self-organized systems, in *2008 Second IEEE International Conference on Self-Adaptive and Self-Organizing Systems (SASO)* (IEEE Computer Society, Los Alamitos, CA, USA, 2008) pp. 435–444.
- [22] B. Meyer, Optimal information transfer and stochastic resonance in collective decision making, *Swarm Intelligence* **11**, 131 (2017).
- [23] B. Meyer, A. Cedrick, and T. Nakagaki, The role of noise in self-organized decision making by the true slime mold *Physarum polycephalum*, *PLOS ONE* **12**, 1 (2017).

- [24] T. Kadowaki and H. Nishimori, Quantum annealing in the transverse ising model, *Phys. Rev. E* **58**, 5355 (1998).
- [25] H. Stanley, *Introduction to Phase Transitions and Critical Phenomena*, International series of monographs on physics (Oxford University Press, 1987).
- [26] S. Mori, S. Nakamura, K. Nakayama, and M. Hisakado, Phase transition in ant colony optimization, *Physics* **6**, 123 (2024).
- [27] C. Gardiner, *Stochastic Methods: A handbook for the Natural and Social Science, 4th ed.* (Springer, Berlin, 2009).
- [28] D. J. Thouless, P. W. Anderson, and R. G. Palmer, Solution of 'solvable model of a spin glass', *The Philosophical Magazine: A Journal of Theoretical Experimental and Applied Physics* **35**, 593 (1977), <https://doi.org/10.1080/14786437708235992>.